ELSEVIER

Applied Surface Science 195 (2002) 63–73

applied surface science

www.elsevier.com/locate/apsusc

Effect of in situ Pt bottom electrode deposition and of Pt top electrode preparation on PZT thin films properties

B. Vilquin*, G. Le Rhun, R. Bouregba, G. Poullain, H. Murray

Laboratoire CRISMAT/ISMRA, Université de Caen, CNRS UMR 6508, 6 Boulevard du Maréchal Juin, 14050 Caen Cedex, France

Received 12 February 2002; accepted 3 May 2002

Abstract

Highly (1 0 0) oriented Pb(Zr, Ti)O_3 (PZT) thin films have been grown in situ at 500 °C on Pt electrode by rf magnetron sputtering. The Pt bottom electrode has been sputtered in situ and influence of Pt deposition temperature on structural and electrical properties of PZT films have been investigated. The effect of preparation conditions of Pt top electrodes has also been examined. It was found that properties of PZT thin films were strongly dependent on the deposition temperature of the bottom electrode and on both the rf power and plasma composition during the sputtering of the top electrode.

PACS: 81.15.Cd Deposition by sputtering; 77.84.-s Dielectric, piezoelectric, ferroelectric, and antiferroelectric materials; 68.55.-a Thin film structure and morphology

1. Introduction

The high remnant polarization and piezoelectric constants of PZT thin films make them very promising for the preparation of memory and micromechanical devices [1,2]. Their electrical properties are strongly dependent on many parameters, including composition [3,4], crystallographic orientation [5,6] and substrates [7–9]. The integration of PZT thin films in microelectronic devices requires preferentially the use of silicon substrates. However, undesirable diffusion should be avoided at the interfaces between the ferroelectric layer, the electrode and the Si wafer. Indeed, these interactions may lead to degradations of the films properties, such as decrease of both dielectric constant and remnant polarization or pronounced fatigue. The bottom electrode must not chemically interact with the ferroelectric layer, Pt is selected primarily because of its high electric conductivity and good stability at high temperature. Conductive oxide materials such as RuO_2, $LaSrCoO_3$ have been investigated to form the electrodes [10,11]. However, their crystallization temperature above 600 °C together with the use of an oxidizing atmosphere during the deposition don't meet the requirements for their integration in Si integrated circuits. Many researchers (for instance [12–15]) worked on the elaboration of a Pt bottom electrode suitable for use as a substrate. They claimed that degradations in the ferroelectric properties are caused by interactions at the interface and by the roughness of the electrode. As demonstrated for instance by Willems et al. [16] and

* Corresponding author. Tel.: +33-231-452-911; fax: +33-231-951-600.
E-mail address: bertrand.vilquin@ismra.fr (B. Vilquin).

0169-4332/02/$ – see front matter
PII: S0169-4332(02)00554-8

Velu and Remiens [17], Ti may diffuse from the adhesion layer, between Pt and Si, into the electrode during its annealing treatment and the crystallization of PZT films. In order to avoid this diffusion, they proposed to oxidize the Ti layer into TiO_2. Nevertheless, most of these studies were carried out on post-annealed Pt when electrodes processing should preferentially be made in situ for a complete PZT/Pt integration. Effects of top electrode deposition and annealing on the ferroelectric properties have also been reported [18–20]. Ionic bombardment associated to the Pt deposition process may cause damage in PZT films. However, only few studies [21] have been devoted to analyse the influence of top electrode deposited without any post-annealing treatment.

In this paper, the influence of Pt bottom and top electrodes preparation on in situ oriented PZT thin films is analysed. Structural properties of Pt bottom electrode are first investigated for various in situ deposition conditions. Crystalline structure and electrical properties of PZT thin films grown on these different electrodes are then investigated as a function of Pt deposition temperature. Lastly, the sputtering effect of Pt top electrodes on PZT capacitors properties is examined.

2. Experimental

Two hundred and fifty nanometers thick $Pb(Zr_{0.7}Ti_{0.3})O_3$ films were grown in situ at 500 °C by rf sputtering on $Pt/TiO_2/SiO_2/Si$ substrates. TiO_2 and Pt layers were deposited on thermally oxidized Si substrates by rf sputtering at various temperatures ranging from 400 to 600 °C, TiO_2 under a gas mixture of oxygen (5%) and argon (95%) and Pt under a pure argon atmosphere. The TiO_2 interlayer promotes adhesion of the Pt electrode on SiO_2/Si substrate and avoids diffusion of Si in the electrode. The $O_2/(Ar + O_2)$ ratio during Ti sputtering was found to strongly modify crystallization of the Pt layer: in our deposition chamber, an oxygen part of 5% is required to obtain a well crystallization of the Pt electrode. The thickness of TiO_2 and Pt layers of 20 and 180 nm, respectively, were measured with a Dektak profilometer. The deposition conditions of the different Pt electrodes are summarized in Table 1.

Table 1
Deposition conditions of Pt bottom electrodes

	TiO_2 layer	Pt layer
Temperature (°C)	400–600	400–600
Thickness (nm)	20	180
Plasma gas	95% Ar + 5% O_2	Ar
Pressure (Pa)	1.4	1.4
Power density (W/cm^2)	4	3

A very thin TiO_x layer was then grown, prior to PZT deposition, on the Pt electrode by sputtering a Ti target at 500 °C. The sputtering gas was composed of pure Ar and the gas pressure was 1 Pa. We have demonstrated in previous reports [22–24] that this very thin TiO_x layer not only promoted the crystallization of PZT film on platinized Si substrates at 500 °C but also allowed the control of the PZT film texture, which was achieved by monitoring the $O_2/(Ar + O_2)$ ratio during Ti deposition. Highly (1 0 0) oriented PZT films were then grown when Ti was sputtered under a pure argon ambience. In the present work, PZT films were deposited using a multi-target rf sputtering system with a rotating substrate holder and three cathodes. Targets were metallic Pb, Ti and Zr. The plasma atmosphere was a gas mixture of 75% argon and 25% oxygen and its pressure was set at 1.4 Pa. The rf power of each cathode is separately monitored and allows to control the PZT film composition.

Crystallographic properties of PZT films and Pt bottom layers were examined by a Seifert X-ray diffractometer (XRD) using Cu Kα radiation and a four-circles Philips X'Pert diffractometer. Composition and surface morphology were investigated by a scanning electron microscope (SEM) coupled with an energy dispersive spectroscopy (EDS) analysis.

To check for electrical properties, 250 μm × 250 μm Pt top electrodes were deposited under various plasma compositions and different rf powers, at room temperature on PZT samples. Ferroelectric hysteresis loops were observed using a Sawyer–Tower circuit driven at 200 Hz by a sine wave. Capacitance–voltage (C–V) curves and dielectric constants ε_r were determined from small signal capacitance measurements performed at 50 kHz with a 2.5 kV/cm ac field using a Keithley LCZ meter.

3. Structural properties of bottom electrodes and PZT films

3.1. Pt bottom electrodes

The θ–2θ scans (Fig. 1) indicate that the Pt layer exhibits only (1 1 1) oriented grains whatever the deposition temperature. The crystallization increases with the deposition temperature since the intensity of the Pt (1 1 1) line went up with temperature. This fact is confirmed by values of FWHM measured with a rocking curve on the Pt (1 1 1) line which decreased from 6.1 to 4.2° as the temperature is raised from 400 to 600 °C (Fig. 2). The mozaïcity of the Pt grains depends on the substrate temperature and shows a minimum above 550 °C. Fig. 3(a)–(e) displays the surface morphology of the (1 1 1) Pt layers deposited at respectively 400, 450, 500, 550 and 600 °C.

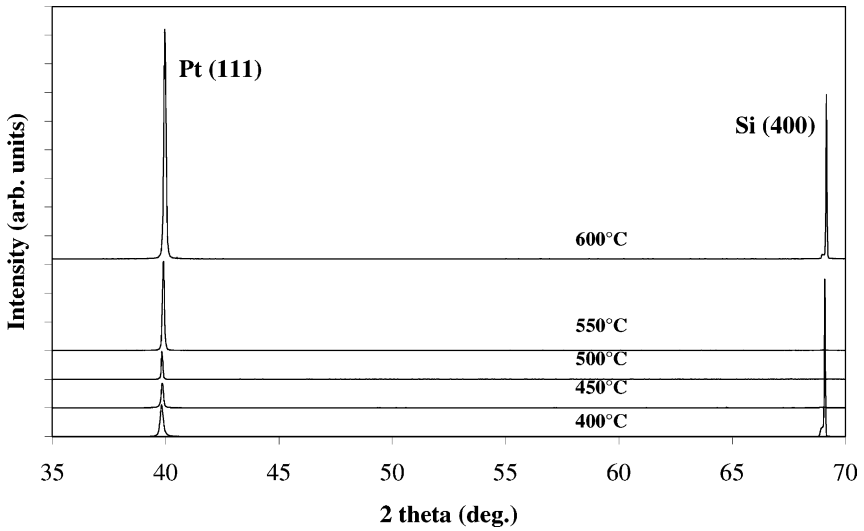

Fig. 1. XRD patterns of Pt layers as a function of deposition temperature.

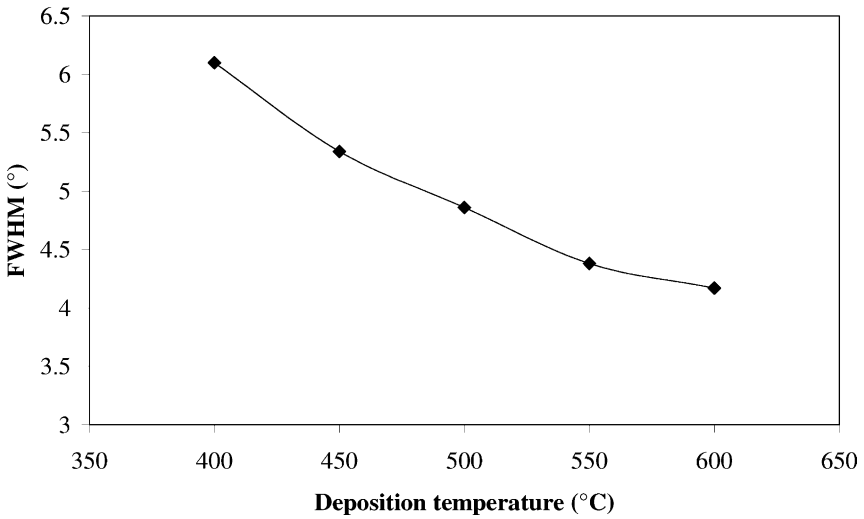

Fig. 2. Values of the (1 1 1) Pt rocking curve with the deposition temperature.

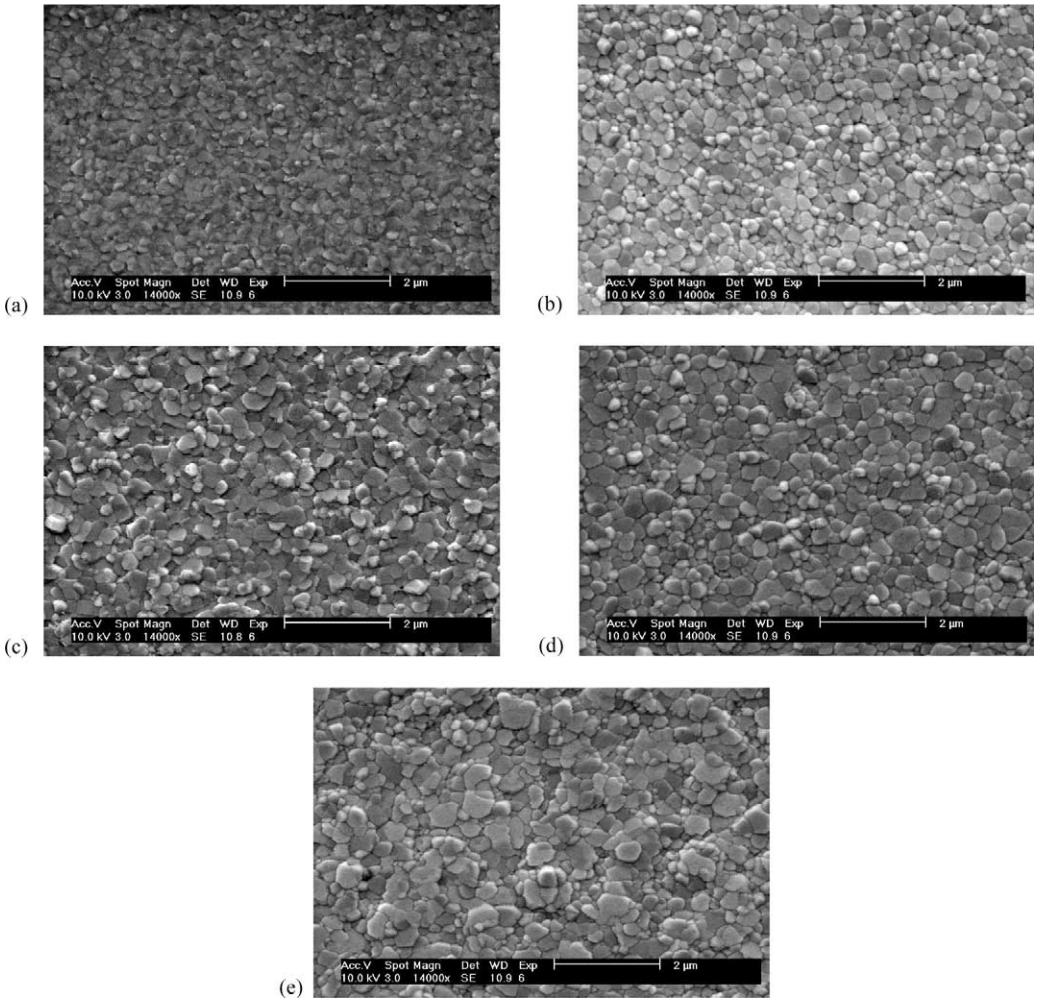

Fig. 3. SEM images of the surface morphology of the different Pt electrodes. The Pt crystallized at: (a) 400 °C, (b) 450 °C, (c) 500 °C, (d) 550 °C, (e) 600 °C.

The grains size increases from 0.2 to 0.5 μm and the surface morphology becomes smoother, as the deposition temperature increases.

3.2. PZT films

Fig. 4(a)–(e) shows the XRD patterns of PZT films deposited during the same run on the various Pt electrodes. The films exhibit only the perovskite phase with no parasitic phase like pyrochlore. The θ–2θ scan of the ferroelectric layer grown on the Pt electrode crystallized at 400 °C is presented Fig. 4(a). In this case, the PZT layer is strongly (1 0 0) oriented with however few (1 1 0) grains. On the other hand, ferroelectric films crystallized on the Pt deposited above 450 °C (see Fig. 4(b)–(e)) present only (1 0 0) orientation. The intensity of (1 0 0) and (2 0 0) lines increases with the deposition temperature of the electrode, which indicates that the PZT layer is better crystallized, even though the PZT deposition was performed under strictly identical conditions. Fig. 5(a)–(c) shows the surface of PZT films grown on Pt electrodes crystallized at 400, 500 and 600 °C. No difference is observed on the SEM images in

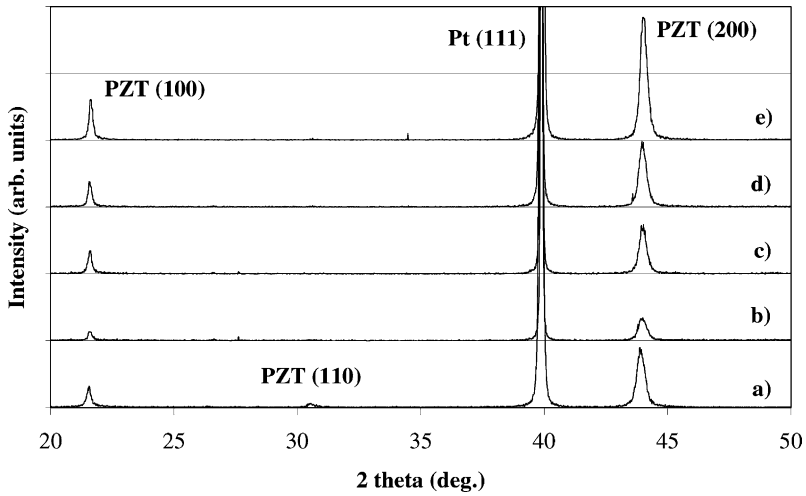

Fig. 4. XRD patterns of PZT films deposited during the same run on Pt electrodes crystallized at: (a) 400 °C, (b) 450 °C, (c) 500 °C, (d) 550 °C, (e) 600 °C.

particular for the grains size and the roughness. In all cases, PZT films microstructure is dense and homogeneous. The rocking-curves performed on the (1 0 0) PZT line show only a slight decrease of the FWHM (Fig. 6), which indicates that the electrode fabrication has only a small influence on the dispersion of grain orientation in the PZT layer for temperature above 450 °C.

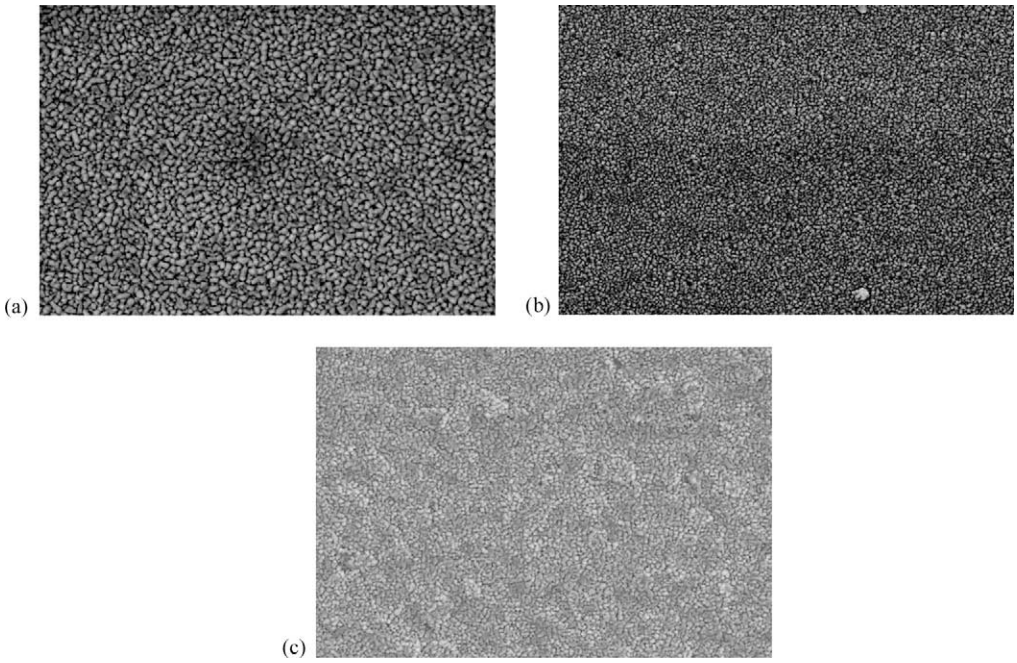

Fig. 5. SEM images of the surface of PZT films sputtered during the same run at 500 °C on Pt electrodes crystallized at: (a) 400 °C, (b) 500 °C, (c) 600 °C.

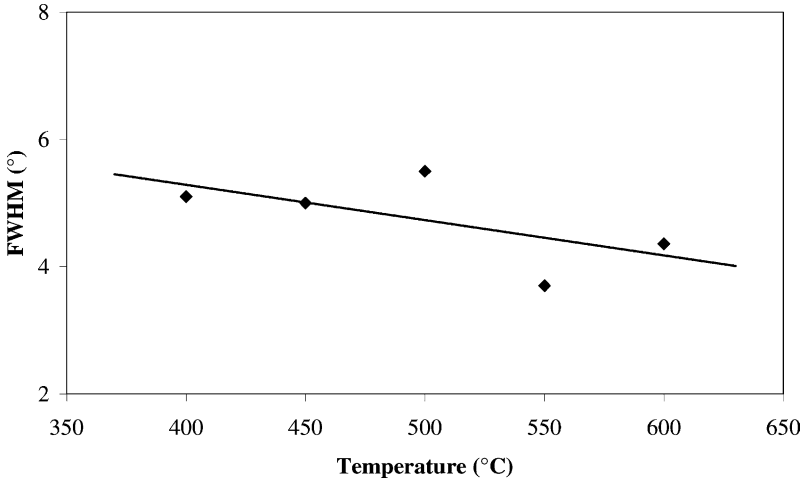

Fig. 6. Values of the (1 0 0) PZT rocking curve with the Pt deposition temperature.

4. Electrical characterization

4.1. PZT films on the various bottom electrodes

Fig. 7(a)–(c) shows three ferroelectric loops measured on PZT films grown on Pt electrode crystallized at 400, 500 and 600 °C, respectively. PZT films present *D–E* loops with a well saturated shape and low coercive field (E_c). However, higher remnant polarizations are obtained when the temperature of the Pt deposition increases, from 8 to 12 μC/cm^2. These values are in accordance with those earlier published for (1 0 0) oriented PZT films. Surprisingly, the coercive field (around 70 kV/cm) is not influenced by the crystallization temperature of the electrode. Values of the remnant polarization, coercive field and dielectric constants of the different samples are given in Table 2. Fig. 8(a)–(e) presents the dielectric constant values extracted from small signal capacitance measurements and Fig. 9 gives the evolution with the frequency of the dielectric constant at 0 V for the different samples. One may clearly observe the

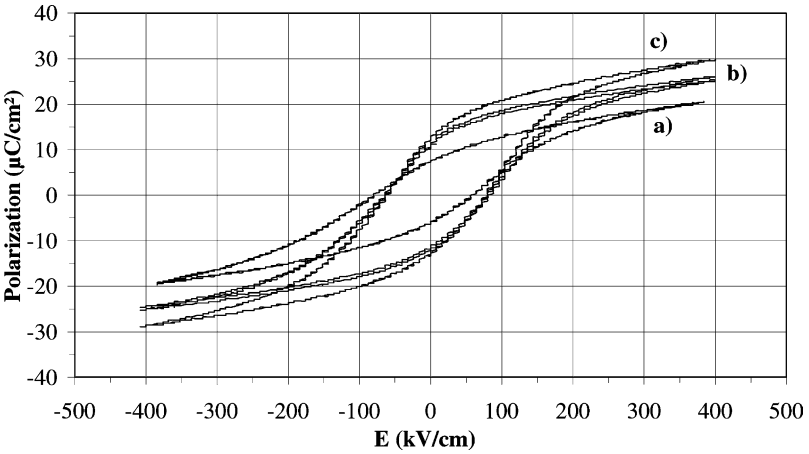

Fig. 7. Polarization loops measured on PZT films deposited during the same run on Pt electrodes crystallized at: (a) 400 °C, (b) 500 °C, (c) 600 °C.

Table 2
Main electrical parameters measured on PZT films as a function of Pt deposition temperature

Pt deposition temperature (°C)	P_r (μC/cm^2)	E_c (kV/cm)	ε_r (0 V and 50 kHz)
400	7.2	76	250
450	9.2	76	280
500	12.0	74	320
550	11.8	68	380
600	13.2	72	400

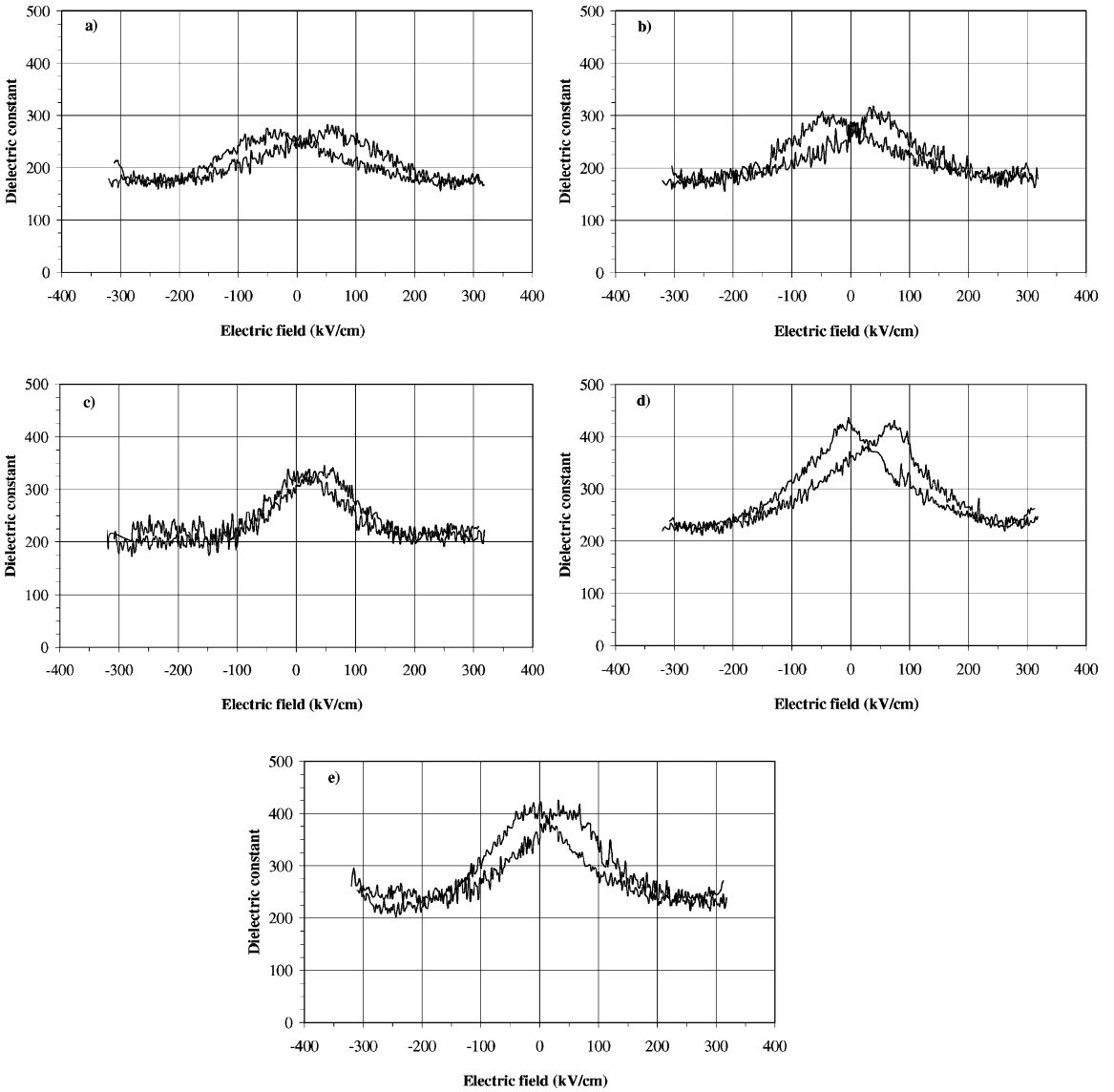

Fig. 8. *C–V* curves of PZT films deposited during the same run on Pt electrodes crystallized at: (a) 400 °C, (b) 450 °C, (c) 500 °C, (d) 550 °C, (e) 600 °C.

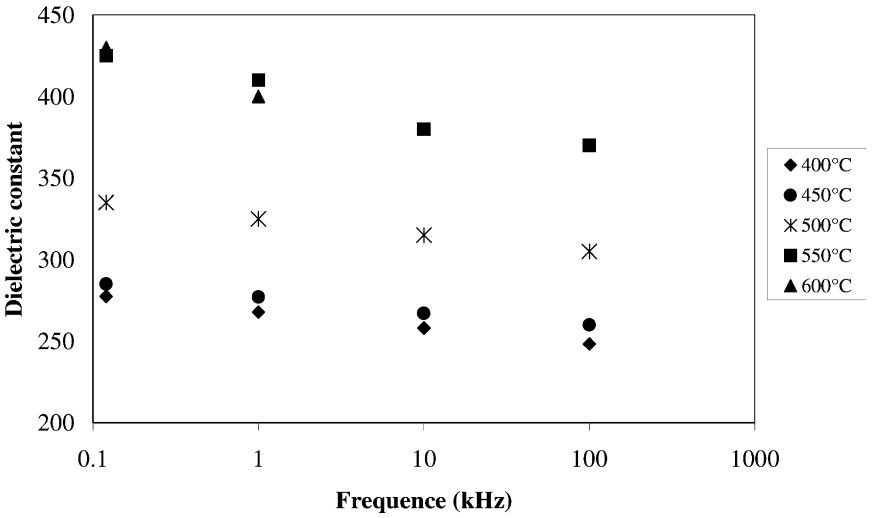

Fig. 9. Variation of the dielectric constant of PZT films as a function of frequency and Pt bottom electrode deposition temperature.

enhancement of dielectric properties with the crystallization temperature of the Pt electrode since the dielectric constants, measured at 0 V, increase from 250 to 400. These values are consistent with those already reported for PZT films with low thicknesses and their decrease with the frequency is typical of PZT films. Values of resistivity as a function of the frequency are also given in Fig. 10. Moreover, it was observed that PZT films grown on Pt electrode crystallized at high temperature, above 550 °C, did not require electrical poling, while at 400 °C an electrical treatment was necessary to observe ferroelectric loops.

It is clear that the Pt crystallization temperature strongly influences the dielectric and ferroelectric properties of PZT films, more especially as all PZT films were grown during the same run. The increase of

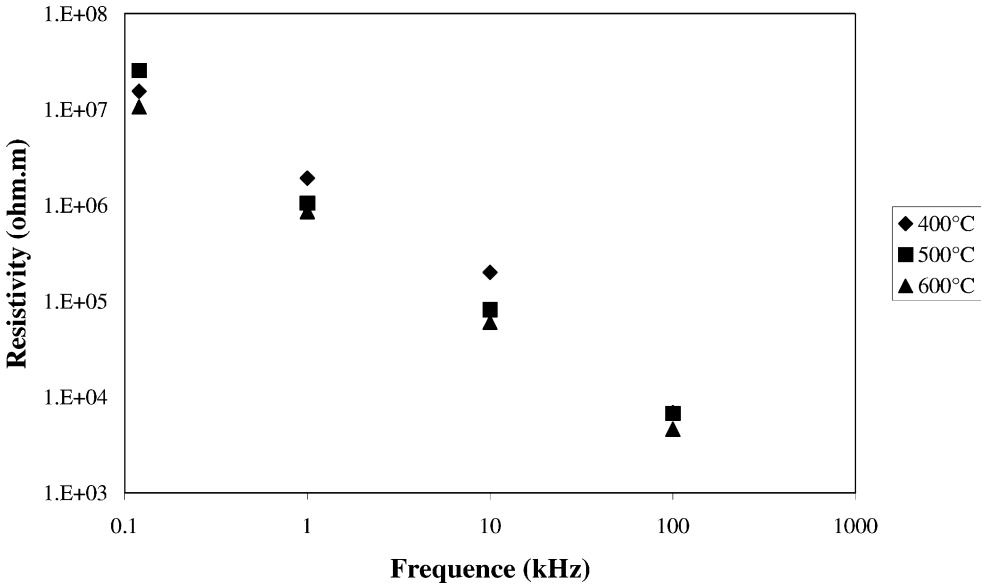

Fig. 10. Variation of the resistivity of PZT films as a function of frequency and Pt bottom electrode deposition temperature.

Table 3
Main electrical parameters measured on PZT films as a function of rf power density and plasma gas during Pt top electrodes deposition

Power density (W/cm^2)	Plasma gaz	P_r (μC/cm^2)	E_c (kV/cm)	ε_r (0 V and 120 Hz)
1.2	Ar	10	94	300
2.4	Ar	12	88	315
2.4	Ar + O_2	12	75	400
3.7	Ar	11	81	340

Pt deposition temperature leads to improvement of both electrode and PZT microstructures, and likely of the interface between Pt and PZT layers. This latter point may result to the reduction of interfacial capacitance arising from possible presence of passive layers taking place at the interface between Pt and PZT layers. The effect of such low dielectric constant interfacial layer, which is known to degrade the apparent dielectric constant and the ferroelectric polarization [25], may be reduced when the Pt is deposited at high temperature. We conclude that properties of PZT films are strongly linked with the preparation conditions of the Pt bottom electrode since the perovskite crystallization and the quality of the interface between PZT and electrodes may be more or less affected according to its deposition temperature.

4.2. PZT films with various top electrodes

Deposition of top electrodes by sputtering is known to cause damage in ferroelectric films because of possible integration of argon ions or creation of oxygen vacancies. Sputtering conditions of Pt top electrodes must therefore be analyzed in view of reducing these detrimental effects.

A PZT film was grown in situ at 500 °C with the conditions summarized in the Section 2 on a Pt electrode deposited at 550 °C. Top electrodes have been sputtered at room temperature on the same PZT film with different rf power density (from 1.2 to 3.7 W/cm^2). The plasma was composed of pure argon and its pressure was fixed at 0.5 Pa. However for the trial at 2.4 W/cm^2, one deposition was carried out by using a plasma of 90% argon and 10% oxygen at the first stage (5 nm) of the Pt deposition. No post-deposition annealing was used after the Pt top electrode sputtering in order to study the effect of the top electrode interface quality on the hysteresis loops.

The main electrical measurements are given in Table 3 and Fig. 11 shows *D–E* loops. One may observe a large spread of electrical values. The best result is obtained when the top electrode is sputtered at 2.4 W/cm^2 under a mixture of argon and oxygen at the

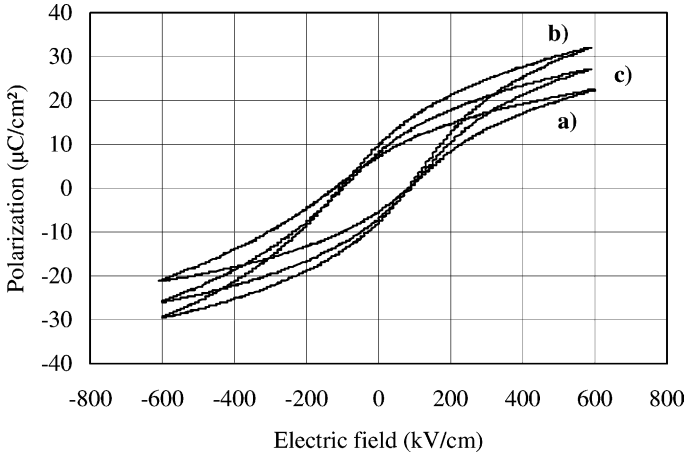

Fig. 11. Polarization loops measured on PZT film with Pt top electrodes deposited at: (a) 1.2 W/cm^2, (b) 2.4 W/cm^2, (c) 3.7 W/cm^2.

first stage of Pt deposition and under pure argon after. A coercive field of 75 kV/cm, a remnant polarization of 12 μC/cm^2 and a dielectric constant (0 V and 120 Hz) of 400 are obtained. Fig. 12 presents hysteresis loop and variations of the dielectric constant as a function of electric field and frequency.

The use of a mixture of argon and oxygen in the plasma gas seems to prevent creation of oxygen

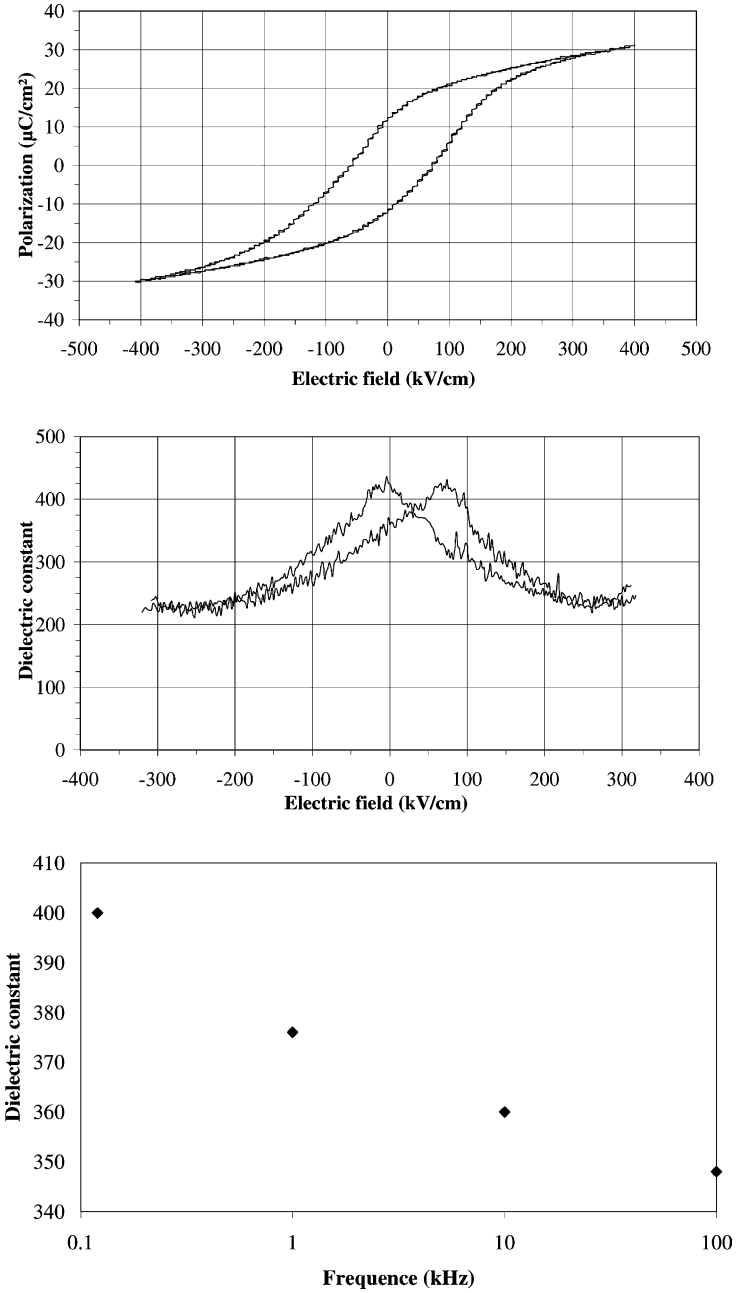

Fig. 12. Polarization loop and variations of the dielectric constant as a function of electric field and frequency for a PZT film with a Pt top electrode sputtered at 2.4 W/cm^2.

vacancies at the surface of PZT films, perhaps caused by the catalystic effect of Pt as suggested by Bursill et al. [10], Niwa et al. [14], and Kushida-Abdelghafar et al. [26]. At high power densities, the deterioration of dielectric and ferroelectric properties may be attributed to damages caused by ionic bombardment for instance due to possible integration of Ar ions at the surface of the film. This may lead to formation of an interfacial passive layer. At low power densities, Ar ions and Pt atoms did not acquire enough energy to allow a strong adhesion of the top electrode on the PZT. A further possible improvement of the top electrode might be to sputter Pt while heating the PZT sample. However, this will impose to etch the Pt to pattern the top electrode since the resist, required for the lift off, would not endure the heating.

5. Conclusion

From results on structural, dielectric and ferroelectric properties of PZT films, two main conclusions may be drawn for both in situ deposition of the bottom electrode and preparation conditions of the top electrode.

Both morphologic structure of the bottom electrode, crystallographic and electrical properties of PZT films are markedly improved when the Pt deposition temperature is increased. The best results were obtained for Pt grown above 550 °C. The temperature of Pt crystallization has therefore a great influence on dielectric and ferroelectric properties of PZT films.

For top electrodes deposited at room temperature, an optimum power density (of 2.4 W/cm^2) was found and a plasma gas composed of a mixture of argon and oxygen during the first stage was required to prevent possible creation of oxygen vacancies and degradation at the surface of PZT films.

These results clearly demonstrated that all the fabrication process of thin metal–ferroelectric–metal capacitors should be carefully controlled to improve their dielectric and ferroelectric properties. In particular, significant improvements are possible by in situ processing of both top and bottom electrodes.

References

[1] J.F. Scott, C.A. Araujo, Science 246 (1989) 1400.
[2] S.L. Swartz, V.E. Wood, Cond. Mater. News 1 (1992) 4.
[3] R. Takayama, Y. Tomita, J. Appl. Phys. 65 (1989) 1666.
[4] K. Sreenivas, M. Sayer, J. Appl. Phys. 64 (1988) 1484.
[5] X. Du, J. Zheng, U. Belegundu, K. Uchino, Appl. Phys. Lett. 72 (1998) 2421.
[6] D.F.L. Jenkins, W.W. Clegg, G. Velu, E. Cattan, D. Remiens, Ferroelectrics 224 (1999) 259.
[7] C.M. Foster, Z. Li, M. Buckett, D. Miller, P.M. Baldo, L.E. Rehn, G.R. Bai, D. Guo, H. You, K.L. Merkle, J. Appl. Phys. 78 (1995) 2607.
[8] C.M. Foster, G.R. Bai, R. Csencsits, J. Vetrone, R. Jammy, L.A. Wills, E. Carr, J. Amano, J. Appl. Phys. 81 (1997) 2349.
[9] S. Hong, H. Bak, I. An, O.K. Kim, Jpn. J. Appl. Phys. 39 (2000) 1796.
[10] L.A. Bursill, I. Reaney, D.P. Vijay, S.B. Desu, J. Appl. Phys. 75 (1994) 1521.
[11] S.G. Ghonge, E. Goo, R. Ramesh, T. Sands, V.G. Keramidas, Appl. Phys. Lett. 63 (1993) 1628.
[12] K. Sreenivas, I. Reaney, T. Maeder, N. Setter, C. Jagadish, R.G. Elliman, J. Appl. Phys. 75 (1994) 232.
[13] E.G. Lee, D.J. Wouters, G. Willems, H.E. Maes, Appl. Phys. Lett. 69 (1996) 1223.
[14] K. Niwa, Y. Kotoka, M. Tomotani, H. Ashida, Y. Goto, S. Otani, Acta Mater. 48 (2000) 4755.
[15] S.T. Kim, H.H. Kim, M.Y. Lee, W.J. Lee, Jpn. J. Appl. Phys. 36 (1997) 294.
[16] G.J. Willems, D.J. Wouters, H.E. Maes, Micro. Eng. 29 (1995) 217.
[17] G. Velu, D. Remiens, J. Eur. Ceram. Soc. 19 (1999) 2005.
[18] I.K. Naik, L.E. Sanchez, S.Y. Wu, B.P. Maderic, Integrat. Ferroelectr. 2 (1992) 133.
[19] K. Ishihara, T. Ishikawa, K. Hamada, S. Onishi, J. Kudo, K. Sakiyama, Integrat. Ferroelectr. 6 (1995) 301.
[20] D.J. Wouters, G. Willems, G. Groeseneken, H.E. Maes, K. Brooks, Integrat. Ferroelectr. 7 (1995) 173.
[21] E.G. Lee, D.J. Wouters, G. Willems, H.E. Maes, Integrat. Ferroelectr. 16 (1997) 165.
[22] R. Bouregba, G. Poullain, B. Vilquin, H. Murray, Mater. Res. Bull. 35 (2000) 1381.
[23] B. Vilquin, R. Bouregba, G. Poullain, M. Hervieu, H. Murray, Eur. Phys. J. AP 15 (2001) 153.
[24] R. Bouregba, G. Poullain, B. Vilquin, H. Murray, Ferrolectrics 256 (2001) 47.
[25] P.K. Larsen, G.J.M. Dormans, D.J. Taylor, P.J. van Veldhoven, J. Appl. Phys. 76 (1994) 2405.
[26] K. Kushida-Abdelghafar, H. Miki, K. Torii, Y. Fujusaki, Appl. Phys. Lett. 69 (1996) 3188.